TU/e EINDHOVEN UNIVERSITY OF TECHNOLOGY

Dependence of Temporal Frequency and Chromaticity on the Visibility of the Phantom Array Effect

Citation for published version (APA):
Kong, X., Vogels, R., Martinsons, C., Tengelin, M. N., & Heynderickx, I. E. J. (2023). Dependence of Temporal Frequency and Chromaticity on the Visibility of the Phantom Array Effect. In *Proceedings of the 30th CIE SESSION* (pp. 347-356). CIE. https://doi.org/10.25039/x50.2023.OP060

Document license:
CC BY-NC

DOI:
10.25039/x50.2023.OP060

Document status and date:
Published: 29/12/2023

Document Version:
Publisher's PDF, also known as Version of Record (includes final page, issue and volume numbers)

Please check the document version of this publication:

• A submitted manuscript is the version of the article upon submission and before peer-review. There can be important differences between the submitted version and the official published version of record. People interested in the research are advised to contact the author for the final version of the publication, or visit the DOI to the publisher's website.
• The final author version and the galley proof are versions of the publication after peer review.
• The final published version features the final layout of the paper including the volume, issue and page numbers.

Link to publication

General rights
Copyright and moral rights for the publications made accessible in the public portal are retained by the authors and/or other copyright owners and it is a condition of accessing publications that users recognise and abide by the legal requirements associated with these rights.

• Users may download and print one copy of any publication from the public portal for the purpose of private study or research.
• You may not further distribute the material or use it for any profit-making activity or commercial gain
• You may freely distribute the URL identifying the publication in the public portal.

If the publication is distributed under the terms of Article 25fa of the Dutch Copyright Act, indicated by the "Taverne" license above, please follow below link for the End User Agreement:

www.tue.nl/taverne

Take down policy
If you believe that this document breaches copyright please contact us at:

openaccess@tue.nl

providing details and we will investigate your claim.

Download date: 10. Aug. 2024

International Commission on Illumination
Commission Internationale de l'Eclairage
Internationale Beleuchtungskommission

OP60

DEPENDENCE OF TEMPORAL FREQUENCY AND CHROMATICITY ON THE VISIBILITY OF THE PHANTOM ARRAY EFFECT

Kong, X., Vogels, R., Martinsons, C., Tengelin, M., Heynderickx, I.

DOI 10.25039/x50.2023.OP060

Pages 347–356 from

CIE x050:2023

Proceedings
of the
30th CIE SESSION
Ljubljana, Slovenia, September 15 – 23, 2023
(DOI 10.25039/x50.2023)

The paper has been presented at the 30th CIE Session, Ljubljana, Slovenia, September 15 – 23, 2023. CIE 2023 conference papers were accepted on the basis of double-blind abstract review. The Proceedings papers are published as supplied by the authors.

© CIE 2023

All rights reserved. Unless otherwise specified, no part of this publication may be reproduced or utilized in any form or by any means, electronic or mechanical, including photocopying and microfilm, without permission in writing from CIE Central Bureau at the address below. Any mention of organizations or products does not imply endorsement by the CIE.

This paper is made available open access for individual use. However, in all other cases all rights are reserved unless explicit permission is sought from and given by the CIE.

CIE Central Bureau
Babenbergerstrasse 9
A-1010 Vienna
Austria
Tel.: +43 1 714 3187
e-mail: ciecb@cie.co.at
www.cie.co.at

DEPENDENCE OF TEMPORAL FREQUENCY AND CHROMATICITY ON THE VISIBILITY OF THE PHANTOM ARRAY EFFECT

Kong, X.[1], Vogels R.[1], Martinsons C.[2], Tengelin M.N.[3], Heynderickx I.[1]
[1] Eindhoven University of Technology, Eindhoven, the Netherlands, [2] Centre Scientifique et Technique du Bâtiment, Saint Martin d'Hères, France, [3] RISE Research Institutes of Sweden, Borås, Sweden
x.kong@tue.nl

DOI 10.25039/x50.2023.OP060

Abstract

The effect of both temporal frequency and chromaticity on the visibility of the phantom array effect has been reported in literature. However, how the visibility changes with the temporal frequency is not consistently answered yet and, therefore, needs additional measurements. As for the effect of chromaticity, literature describes studies with different luminaires (i.e., with different chromaticities and peak wavelengths) and settings (i.e., different intensities and viewing geometry); as a consequence, it is challenging to compare these results directly. Therefore, we investigate the effect of temporal frequency on the visibility of the phantom array effect again, but with a special interest in how the peak frequency changes with chromaticity. The results of our experiment show a bandpass-shaped sensitivity function for the phantom array effect with a peak at 600 Hz, without significant change as a function of the chromaticities used in our experiment. However, the peak sensitivity value is found to be higher with red light than with green and white light.

Keywords: Temporal Light Modulation, Temporal Light Artefact, The Phantom Array Effect, Psychophysics, Visual Perception, Contrast Sensitivity Function

1 Introduction

The nearly instantaneous responses of light-emitting diodes (LEDs) to changing currents provoke the perception of so-called temporal light artefacts (TLAs), amongst which are flicker, the stroboscopic effect, and the phantom array effect. Those TLAs are defined in the technical report CIE 249:2022 (CIE, 2022). More specifically, the phantom array effect is defined as the change in perceived shape or spatial layout of objects, induced by a light stimulus whose luminance or spectral distribution fluctuates with time, for a non-static observer in a static environment. The term "non-static" here means that the observer moves their eyes by making saccades. The phantom array effect is most easily observed in low-light situations; typically, people observe the artefact when driving at night behind a vehicle with LED-based (and usually, time modulated) rear lights. Models that predict the visibility of flicker (i.e., FVM, the Flicker Visibility Measure) and the visibility of the stroboscopic effect (i.e., SVM, the Stroboscopic Visibility Measure) are described in literature (Perz *et al.*, 2017, 2018; Perz, 2019; CIE, 2022) and have been widely applied since then. For the phantom array effect, however, no standardized model that predicts the visibility threshold is available yet. Miller et al. (2023) collected visibility threshold data for the phantom array effect by using a rating scale and checked how well SVM could predict the visibility of the phantom array effect. The conclusion is that a separate metric is needed since SVM only exhibited a very weak correlation with the visibility of the phantom array effect.

A detailed literature review on the phantom array effect (CIE, 2022) reported psychophysical studies in which various variables were systematically investigated. It showed that the visibility of the phantom array effect depends on 1) individual characteristics, such as age, gender, and saccade speed (Wang *et al.*, 2017; Kang *et al.*, 2022); 2) characteristics of the light modulation, such as time-averaged luminance (Park *et al.*, 2020), temporal frequency (Wang *et al.*, 2017, 2021; Yu *et al.*, 2018; Yan *et al.*, 2019; Miller *et al.*, 2023), modulation depth (Miller *et al.*, 2023), waveform (Yu *et al.*, 2018; Miller *et al.*, 2023), duty cycle (Miller *et al.*, 2023), and chromaticity of the light source (Yu *et al.*, 2018; Park *et al.*, 2020; Kang, Kim, *et al.*, 2023); and 3)

characteristics of the viewing geometry like foveal or peripheral viewing, light source size (Park *et al.*, 2020) and spatial distribution, saccade amplitude (Wang *et al.*, 2017), and relative motion of the light source to the observer (Lee *et al.*, 2018).

A provisional model of the visibility of the phantom array effect for a point light source based on the spatial contrast sensitivity function (CSF) was described in CIE 249:2022 (CIE, 2022); it predicted a sensitivity peak at around 1 000 Hz. Some experimental investigations, however, showed a peak at about 600 Hz (Yu *et al.*, 2018), or a peak between 500 Hz and 1 000 Hz (Miller *et al.*, 2023); while others concluded that the visibility decreased as the temporal frequency increased (Vogels and Hernando, 2012) and that the phantom array effect was even visible at very high frequencies of above 15 kHz (Kang, Lee, *et al.*, 2023). To get a better understanding of these discrepancies and to collect more data, we performed new measurements on the frequency dependency of the visibility threshold of the phantom array effect.

Since both the spatial and temporal contrast sensitivity function are known to be colour-dependent (Díez-Ajenjo and Capilla, 2010), also the effect of chromaticity on the visibility of the phantom array effect is expected. This dependency has been reported in multiple studies. Yu *et al.* (2018) found that the sensitivity to the phantom array effect is higher for red and white light than for blue light, while no significant difference was found between red and white light. Park *et al.* (2020) also reported that the sensitivity to red and green light was higher than to blue light. Kang et al. (2023) found a significant interaction of chromaticity with temporal frequency, such that the change in visibility of the phantom array effect with chromaticity of the light was only significant for some frequencies. In general, the published research shows that the visibility is higher for green LEDs than for blue LEDs, and higher for warm white LEDs than for the cool white LEDs. In these studies, however, different luminaires (i.e., with different chromaticities and peak wavelengths) and settings (i.e., different intensities and viewing geometry) were used, which makes it challenging to compare all results directly. Hence, we decided to measure the temporal frequency dependency of the phantom array effect for three different coloured light sources.

2 Methods

The experiment was designed to measure the visibility threshold of the phantom array effect at various temporal frequencies and for different chromaticities of the light. To do so, a two-interval forced-choice (2IFC) task was used: participants were instructed to view two sequentially presented stimuli (i.e., a reference stimulus that was driven with a direct current (DC) and a test stimulus that was temporally modulated with a sinusoidal waveform) and indicate in which of the two stimuli the phantom array effect was observed. A Bayesian adaptive psychophysical procedure named QUEST+ (Watson, 2017), implemented as a MATLAB Toolbox (Brainard, 2017), was used to change the modulation depth of the sinusoidal waveform in the next stimuli pair based on the participant's previous response(s). The resulting data were fitted to determine the visibility threshold (expressed as modulation depth varying between 0 (i.e., DC light) and 100 %). Details of the experimental setup, stimuli, method and analysis are given below.

2.1 Experimental Setup

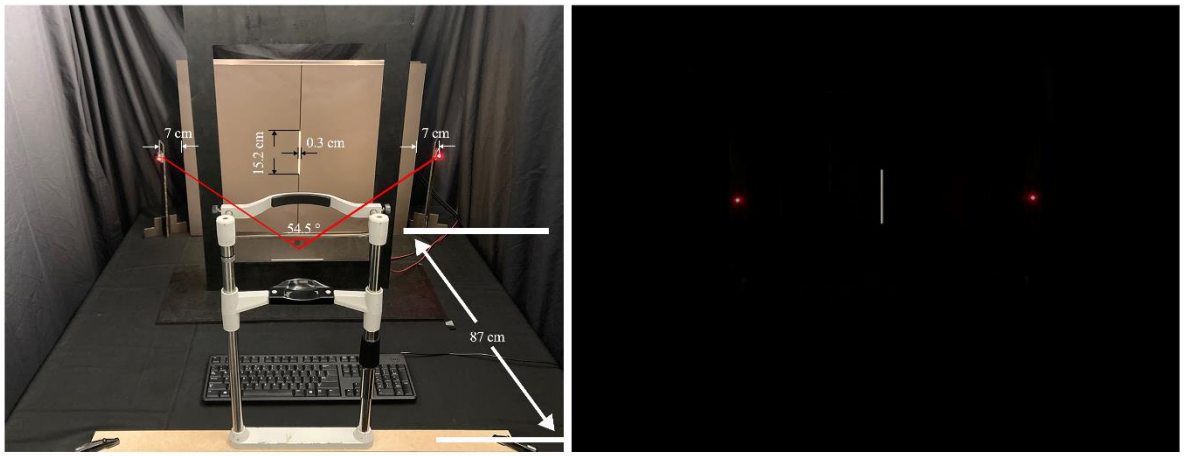

Figure 1 – Experimental setup with laboratory light ON (left) and OFF (right)

The experimental setup is shown in Figure 1. The light source is a customized luminaire that is described elsewhere (Perz, 2019). It consists of 8 rows of LUXEON Rebel LEDs: 4 rows with a CCT of 2 700 K, and 4 rows with a CCT of 6 500 K (not used in the current experiment). A diffusor consisting of multiple layers of filters (Lee 216 White Diffusion) is installed at the frontside of the luminaire to mask the visibility of the individual LEDs, thus improving the uniformity of the light source. A luminance non-uniformity of 14 % (warm white), 23 % (red) and 24 % (green) was measured vertically, using a spectroradiometer (JETI Specbos 1201).

To control the light output (i.e., temporal frequency and modulation depth), a programmable waveform generator (KEYSIGHT Agilent 33522B Series) is used and controlled via TCP/IP protocol by a laptop running MATLAB R2021a. An electronic load (Agilent N3300A) is used to drive the LEDs with a linear current-to-voltage curve. The colour of the light is changed by placing a red filter or a green filter (Lee Colour Filter Set PAR56) in front of the light source. The spectral radiance of the coloured lights and the warm white light, measured at a luminance of 50 cd·m^{-2}, are shown in Figure 2. The corresponding CIE *x*, *y* coordinates of all three light sources are given in Table 1.

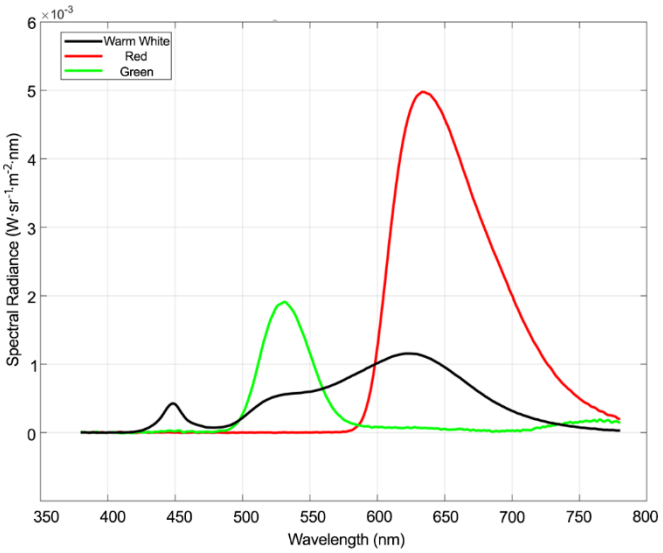

Figure 2 – The spectral radiance of the coloured lights and the warm white light measured at a luminance of 50 cd·m^{-2}

Table 1 – CIE *x*, *y* coordinates of the light sources

	x	*y*
Red	0,689 2	0,309 7
Green	0,244 4	0,696 1
Warm white	0,472 5	0,414 8

The luminaire is placed behind a thin vertical slit made from black foam boards. The slit has a size of 0,3 cm (width) by 15,2 cm (height), corresponding to a visual angle of 0.2° (horizontally) × 10° (vertically) when being viewed by the participants at a distance of 87 cm. To limit head movements of the participants, a chin rest is used. In addition, two low-intensity red LEDs are installed next to the stimulus area to facilitate the participants in making consistent saccades with an amplitude of 55° across the light source. The red chromaticity of the LEDs is chosen intentionally to avoid altering light adaptation conditions (Hecht and Hsia, 1945).

2.2 Stimuli

To measure the visibility threshold of the phantom array effect as a function of temporal frequency, waveforms sinusoidally fluctuating in luminance are generated at six frequencies

around the expected peak sensitivity (Vogels and Hernando, 2012; Yu *et al.*, 2018; Yan *et al.*, 2019; Wang *et al.*, 2021): 80 Hz, 300 Hz, 600 Hz, 900 Hz, 1 200 Hz, and 1 800 Hz. In this experiment, all three light sources have a constant (temporally averaged) luminance level of 50 cd·m^{-2}.

Subsequent stimuli vary in their modulation depth (MD), defined as the Michelson contrast:

$$MD = \frac{L_{\max} - L_{\min}}{L_{\max} + L_{\min}} \tag{1}$$

with L_{max} and L_{min} being the maximum and minimum luminance in the waveform, respectively. These stimuli are paired with a reference stimulus, always DC driven to a luminance of 50 cd·m^{-2}. The test stimulus and reference stimulus are shown sequentially. Whether the reference or test stimulus is shown first is randomized, but with the constraint that the reference is shown first for half of all pairs.

As prescribed in (Watson, 2017), the modulation depth as expressed in Equation (1) needs to be transformed to a logarithm scale (i.e., in dB) for its use in the QUEST+ method; hence we used:

$$s_i = 20 \times \log_{10} MD_i \tag{2}$$

with MD_i representing the *i*-th stimulus in the linear space (so, the MD as defined in (1)), and s_i represents the *i*-th stimulus in dB.

2.3 Experimental Conditions

To minimize eye fatigue of the participants, a fractional factorial 3 (colour) × 6 (temporal frequency) within-subject design was adopted, in which all participants were presented with three frequencies and two colours, thus six conditions in total, as shown in Table 2. The letters R, G and W refer to red, green and warm white light, respectively. A fixed number of 30 trials per condition was used, resulting in 180 (i.e., 2 colours × 3 frequencies × 30 trials) paired comparisons for each participant.

Table 2 – The fractional factorial 3 (colour) × 6 (temporal frequency) mixed design

Participant ID	Colours	Frequencies (Hz)		
1	RG	300	900	1 200
2	GR	300	1 200	1 800
3	RG	300	600	900
4	GR	80	600	1 200
5	RG	600	1 200	1 800
6	GR	80	900	1 200
7	RG	80	300	900
8	WR	80	600	900
9	RW	80	300	1 800
10	WR	80	600	1 800
11	RW	300	600	1 800
12	WR	80	900	1 800
13	RW	80	300	1 200
14	WR	600	900	1 200
15	GW	80	1 200	1 800

16	WG	900	1 200	1 800
17	GW	300	900	1 800
18	WG	80	300	600
19	GW	300	600	1 200
20	WG	600	900	1 800

2.4 Procedure

The experimental protocol was approved by the Ethical Review Board (ERB) of the Eindhoven University of Technology. All participants were recruited either from the university's participant database or from the experimenters' network. The selection criteria were aged between 18 and 45 years, a visual acuity higher than 0,65 (measured with the Landolt-C test at 5 meters distance), no colour deficiency (measured with the Ishihara test), and no history of migraine or epilepsy.

Before the start of the experiment, the recruited participants were first instructed to read and sign the informed consent form. To ensure the participants were qualified to join the experiment, colour deficiency and visual acuity were measured. Participants who did not pass the criteria were excluded from further participation, and were financially compensated for the efforts to come to the lab. Subsequently, the Leiden Visual Sensitivity Test (Perenboom *et al.*, 2018) and the Pattern Glare Test (Evans and Stevenson, 2008) were carried out to get further information about the participant's sensitivity to light and patterns in general. After those tests, the light in the laboratory (i.e., ceiling light) was turned off, so that the participants could adapt to the light condition of the experiment. In this light condition, the illuminance at the eyes was 0,7 lx with the light source turned on.

The participants were seated in front of the experimental set-up and were given an explanation about the phantom array effect, and were provided with instructions for the experiment. Before the start of the actual experiment, the participants were presented with two pairs of stimuli (i.e., two pairs of a test versus reference stimulus) to familiarize themselves with the phantom array effect and the task at hand. Participants were instructed to make several rapid horizontal saccades between the two red LEDs during both intervals (of a pair of stimuli) and were then asked to indicate at which interval the phantom array effect was observed. The participants were facilitated with audio cues, i.e., computer-generated voice instructions as "First stimulus", "Second stimulus", "Input recorded", "Invalid input, please input again". After hearing "First stimulus", the participants were asked to make several saccades. Four seconds later, the instruction "Second stimulus" was given, and the participants had to make several saccades again. After having seen both stimuli, they were instructed to use the *left arrow* key to indicate that the phantom array effect was observed during the first interval, and the *right arrow* key to indicate that the phantom array effect was observed during the second interval. Specifically, they were told that the phantom array effect could be observed in only one of them, and that they had to guess when they didn't see the phantom array effect at all. The first pair of stimuli was an easy one, where the phantom array effect was expected to be clearly visible (MD of 95 % at 600 Hz). Participants who were unable to identify the phantom array effect, even after additional explanation and practice, were excluded from the experiment, and also given financial compensation for their effort to come to the lab. Then a more difficult pair of stimuli (MD of 5 % at 600 Hz) was presented to give the participants a realistic idea of how difficult the task could become. For the actual experiment, the same procedure was used, only the red LED indicators (to guide the saccades) were turned off to avoid distraction.

The experiment was divided into two blocks, as shown in Table 2, with each block containing one colour and three temporal frequencies. Each block took about fifteen minutes. In the first block, one of the three colour filters was placed in front of the light source and the three frequencies that the participant was assigned to were presented in an intermingled order. After all trials were conducted, the participant was given a short break during which the colour filter was replaced by another one. Moreover, some demographics were collected during the break, such as the participant's age, whether the participant had corrected vision and their knowledge about light and lighting research. Additionally, participants were asked about their level of eye fatigue and tiredness in general. In case they felt fine, the next block was started. After the

second block was finished, the participants conducted a final questionnaire about the experiment, how they experienced the phantom array effect, and their level of fatigue. Afterwards, they received their financial compensation.

2.5 Participants

Twenty participants (11 male, 9 female), aged between 19 and 32 years old (mean = 24,2, std. = 3,4), with diversity in ethnic backgrounds, signed up for the experiment. No participant was excluded due to insufficient visual acuity or due to colour deficiency. In addition, no participant was excluded for not seeing the phantom array effect at 600 Hz with a modulation depth of 95 %. The participants spent between 27 and 46 minutes in the laboratory to finish the 180 trials.

3 Results

3.1 Calculation of Visibility Thresholds and Sensitivities

The data collected in the experiment can be plotted in a graph of the percentage of correct responses as a function of modulation depth, per frequency, colour and participant. Through the data in each graph, a so-called psychometric function can be fitted. We chose the Weibull cumulative distribution function as the psychometric function to fit our data, and used the maximum likelihood method provided by the MATLAB toolbox (Brainard, 2017) to perform the fitting. The Weibull cumulative distribution function has the following general form:

$$q = 1 - lapse + (guess + lapse - 1) \times \exp(-10^{(slope \times s - threshold)/20}) \quad (3)$$

where

q	is the percentage of correct responses;
s	is the stimulus intensity (i.e., in our case, the modulation depth, in dB, computed using Equation (2));
$guess$	is 0,5 (i.e., assuming a 50 % chance for a correct response when a participant guesses in a 2IFC task);
$lapse$	is 0,02 (i.e., assuming a 2 % chance for a participant to press the wrong key);
$slope$	is the slope of the psychometric function (which we fixed in our fitting to 3);
$threshold$	is the estimated threshold in dB.

The visibility threshold is defined by the 75 % (i.e., the mid-point between the guessing probability of 50 % and the certainty level of 100 %) correct responses point on the psychometric curve. The psychometric functions for all the participants, frequencies and colours are shown in Figure 3.

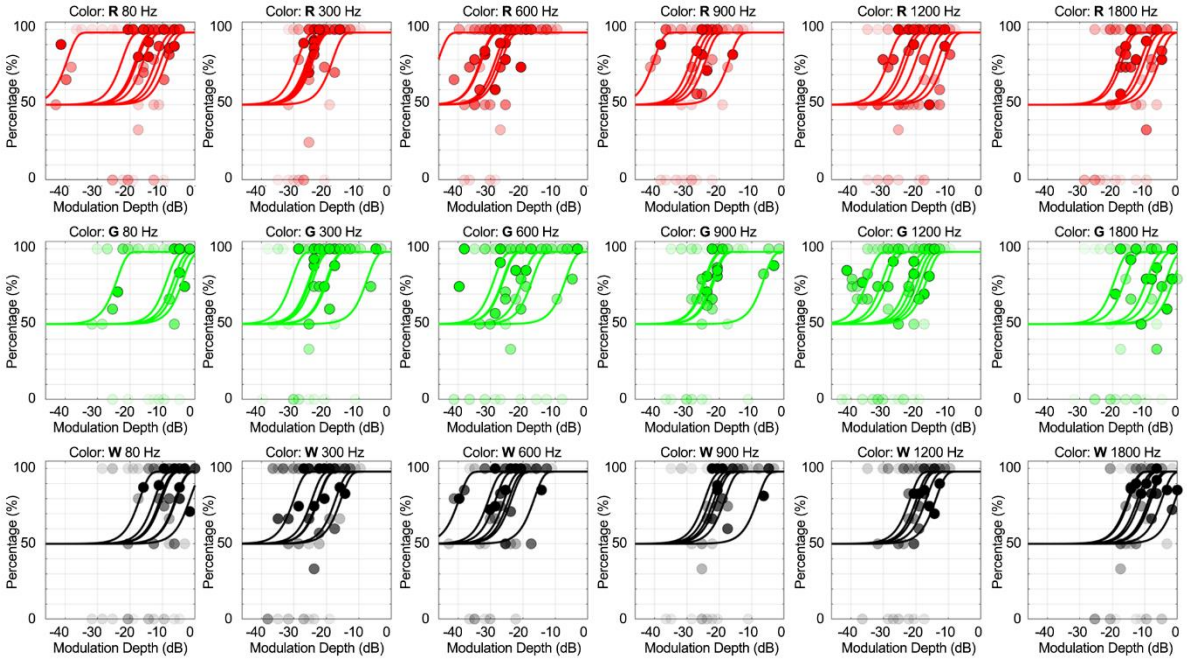

Figure 3 – The psychometric functions, with the y-axis representing the percentage of correct responses and the x-axis representing the modulation depth in dB, for all the participants (collected in one graph) per frequency (increasing in subsequent columns) and colour (red (R) for the top row, green (G) for the middle row, and warm white (W) for the bottom row).

The sensivity is often defined as the reciprocal of the visibility threshold in linear space. Thus the sensitivity to the phantom array effect is expressed as follows:

$$S = \frac{1}{10^{threshold/20}} = 10^{-threshold/20} \tag{4}$$

where

S is sensitivity to the phantom array effect;
$threshold$ is the estimated threshold in dB, using Equation (3).

3.2 Effect of Chromaticity and Frequency on the Visibility Thresholds

Through the fitting procedure described above, we determined in total 120 thresholds (= 20 participants × 2 colours × 3 frequencies), and transformed them into sensitivities. The resulting sensitivity as a function of frequency, averaged over all 20 participants, is given in Figure 4, with the error bars representing the 95 % confidence interval (CI) around the mean. Figure 4 clearly illustrates that the mean sensitivity values are higher at the medium frequencies, with the highest value found at 600 Hz for red (with a mean MD threshold of less than 3 %) and warm white light (with a mean MD threshold of less than 5 %), while the highest value is at 1 200 Hz for green light (with a mean MD threshold of 7 %). Sensitivities are substantially lower at the two far ends of the measured frequency range with averaged MDs at least a factor of 4 higher at both 80 Hz and 1 800 Hz, for all three chromaticities. The black line through the mean sensitivity values is a 3rd-order polynomial fit, as was also used in (Wooten *et al.*, 2010) when modelling the temporal contrast sensitivity function (TCSF). The chi-square values for the three fits are 0,653, 0,897 and 0,413 for red, green and warm white light respectively, indicating that all three fits pass the criterion for goodness of fit at the 0,05 significance level. These fits suggest that despite the deviation for the mid-range frequencies of the green light, the peak sensitivity of the phantom array effect is around 600 Hz, independent of the chromaticity of the light for the colours used in our experiment.

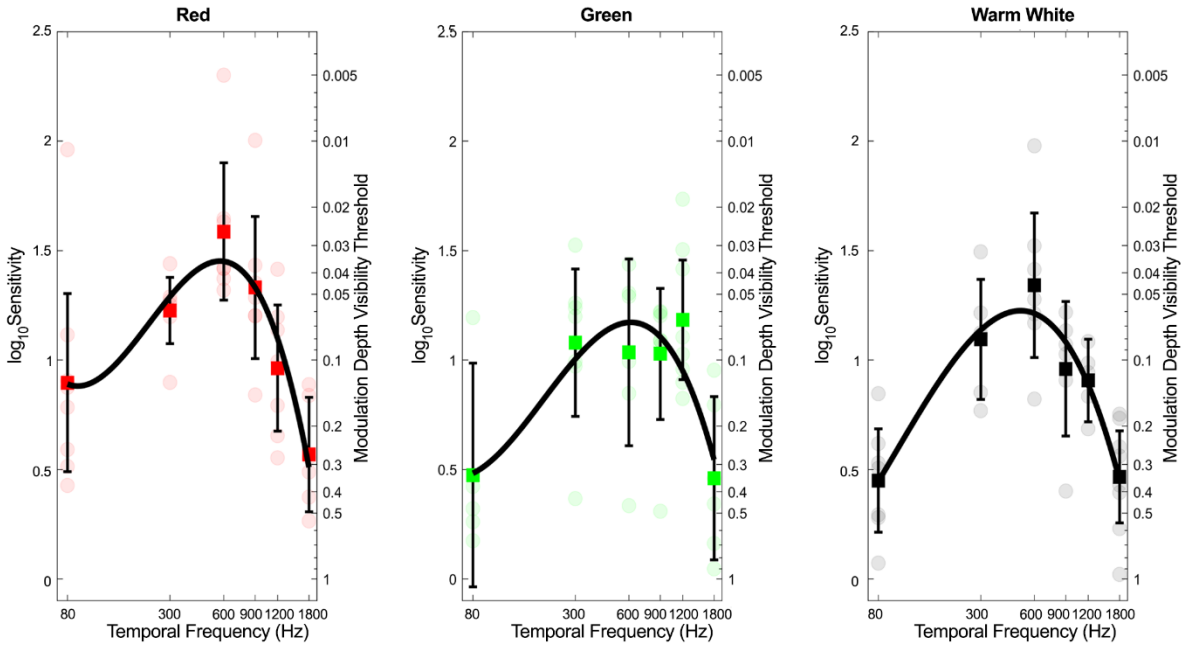

Figure 4 – The sensitivity to the phantom array effect for the three colours. The y-axis on the left represents the logarithm of the sensitivity (as determined with equation (4)), while the y-axis on the right represents the visibility threshold in MD on a logarithmic scale. The x-axis represents temporal frequency in Hz, plotted on a logarithmic scale. The solid lines are third-order polynomial fits.

In order to test the overall effect of *Colour* and *Frequency* on the visibility of the phantom array effect, a linear mixed model (LMM) analysis is performed using IBM SPSS Statistics (Version 28), with logarithmic transformed sensitivity values (i.e., $\log_{10}S$) as the dependent variable, colour and temporal frequency as fixed independent variables. The interaction term between those two variables and a random intercept for *Participant* are also included. The resulting p-values are obtained from a Type III sum of squares. The results of the LMM analysis show a significant effect of *Colour* (F(2, 110,286) = 4,256, p = 0,017), a significant effect of *Frequency* (F(5, 107,816) = 36,178, p < 0,001), and also a significant interaction between *Colour* and *Frequency* (F(10, 101,451) = 2,445, p = 0,012). In addition, there is a significant effect of intercept (F(1, 19,333) = 359,087), p < 0,001), which shows a substantial individual difference.

4 Discussion and Conclusion

Our results show an inverted U-shaped bandpass sensitivity function for the phantom array effect as a function of temporal frequency for all three chromaticities used in the experiment. The 3rd-order polynomial fit indicates a peak sensitivity at a temporal modulation of 600 Hz in all three cases. This finding is in line with earlier results of (Yu *et al.*, 2018; Miller *et al.*, 2023). The fitted curves look similar across the three chromaticities used. However, the peak sensitivity is higher for red than for green and white. The MD visibility threshold is about 3 % for red, whereas it is 6-7 % for green and white. In addition, the low-frequency slope is not as steep for the red colour, compared with the green and warm white colours. It means than the phantom array effect is more visible at low frequencies for the red colour than for green and white colours. The curve for the green chromaticity seems to fit the actual data least, since we measured on average a more or less constant sensitivity between 300 and 1 200 Hz. At this point, it is not fully clear whether this plateau in the data is real, or coincidental measurement noise.

The peak we found differs from the provisional model presented in CIE 249:2022, in which the sensitivity peaks around 1 000 Hz for an averaged luminance of 1 000 $cd \cdot m^{-2}$. In our study, the luminance is 50 $cd \cdot m^{-2}$, which might explain the discrepancy partially. In addition, one can wonder whether a 3rd-order polynomial fit sufficiently reflects the underlying visual processing mechanism of observing the phantom array effect. Other fitting functions, such as Barten's model (Barten, 2003) used in CIE 249:2022, should be carefully evaluated and compared as well. In addition, since the phantom array effect is a spatiotemporal visual phenomenon, modelling its sensitivity as a function of temporal frequency alone clearly has its limitations; expressing the sensitivity as a function of a spatially transformed variable (i.e., when the saccade speed is known) seems more appropriate.

Figure 4 and the statistical analysis in terms of sensitivity indicate that the visibility threshold of the phantom array effect is not only dependent on the frequency of the modulated light, but also on the chromaticity of the light. Also this is in line with earlier findings in literature (Yu *et al.* (2018); Park *et al.* (2020); Kang et al. (2023)), although literature mainly reported differences between red/green light and blue light, and not so much between red, green and white light mutually. Our results suggest that the spectral distribution of the light should be included in models predicting the visibility threshold of the phantom array effect.

Substantial individual differences in sensitivity to the phantom array effect are found as well. These individual differences seem to be larger at 80 Hz and 1 800 Hz than at the other frequencies for both red and warm white light. In addition, the individual differences are larger for green light than for the other two chromaticities. These observations suggest that observing the phantom array effect consistently is more difficult at those two frequencies and for the green light.

There are several limitations of this study worth mentioning. First, the experimental conditions were not completely evenly distributed due to the fractional factorial design. This means that, e.g., 80 Hz does not occur as often with the green colour filter (5 times) as with the red colour filter (8 times). Even though completely evenly distributed conditions would not be possible with the number of participants and the number of conditions, a more even distribution should be aimed for in future, for example, using a full within-subject design. Second, though the participants did not report the vertical non-uniformity of the slit, a deviation of up to 24 % in luminance was present across the slit. Thus, a more uniform light source, for example, using an integration sphere, is recommended for future studies.

5 Acknowledgements

This study was part of the HTI (Human-Technology Interaction) Research Project and was partially supported by the Human-Technology Interaction (HTI) group at Eindhoven University of Technology (TU/e). In addition, the study was executed within the MetTLM-project (i.e, Metrology for Temporal Light Modulation; 20NRM01) and received funding from the EMPIR (European Metrology Programme for Innovation and Research) programme co-financed by the Participating States and from the European Union's Horizon 2020 research and innovation programme.

The authors would like to thank Małgorzata (Gosia) Perz, Walter Willaert, and Pieter Seuntiens from Signify, and Zoe Karamanide, Nikolina Molnar, and Nasir Abed from the lab support team at TU/e, for their professional and excellent help with the experimental setup. The authors would also like to acknowledge other two master students, Anne van Staveren and Myrthe van Geest, from the HTI Group at TU/e, for conducting part of the experiments and contributing to the statistical analysis.

References

Barten, P.G.J. (2003) ‘Formula for the contrast sensitivity of the human eye’, in Y. Miyake and D.R. Rasmussen (eds), pp. 231–238. Available at: https://doi.org/10.1117/12.537476.

Brainard, D.H. (2017) *mQUESTPlus: A Matlab implementation of QUEST+*. Available at: https://github.com/brainardlab/mQUESTPlus.

CIE (2022) *Visual Aspects of Time-Modulated Lighting Systems*. Available at: https://doi.org/10.25039/TR.249.2022.

Díez-Ajenjo, M.A. and Capilla, P. (2010) ‘Spatio-temporal contrast sensitivity in the cardinal directions of the colour space. A review’, *Journal of Optometry*, 3(1), pp. 2–19. Available at: https://doi.org/10.3921/joptom.2010.2.

Evans, B.J.W. and Stevenson, S.J. (2008) ‘The Pattern Glare Test: a review and determination of normative values’, *Ophthalmic and Physiological Optics*, 28(4), pp. 295–309. Available at: https://doi.org/10.1111/j.1475-1313.2008.00578.x.

Hecht, S. and Hsia, Y. (1945) ‘Dark Adaptation Following Light Adaptation to Red and White Lights*1’, *Journal of the Optical Society of America*, 35(4), p. 261. Available at: https://doi.org/10.1364/JOSA.35.000261.

Kang, H. *et al.* (2022) ‘Saccadic Eye Movement Speed Can Explain the Large Variations in Phantom Array Effect Visibility’. Available at: https://doi.org/10.21203/rs.3.rs-2230754/v1.

Kang, H., Lee, C.-S., *et al.* (2023) ‘Phantom array effect can be observed above 15 kHz in high speed eye movement group for high luminance warm white LED’, *Lighting Research & Technology*, p. 147715352211473. Available at: https://doi.org/10.1177/14771535221147312.

Kang, H., Kim, J., *et al.* (2023) ‘Visibility of the phantom array effect at different LED colour temperatures under high-frequency temporal light modulation’, *Lighting Research & Technology*, 55(1), pp. 36–46. Available at: https://doi.org/10.1177/14771535221101558.

Lee, C.-S. *et al.* (2018) ‘Phantom array and stroboscopic effects of a time-modulated moving light source during saccadic eye movement’, *Lighting Research & Technology*, 50(5), pp. 772–786. Available at: https://doi.org/10.1177/1477153517693468.

Miller, N. *et al.* (2023) ‘Phantom array and stroboscopic effect visibility under combinations of TLM parameters’, *Lighting Research & Technology*, p. 147715352311699. Available at: https://doi.org/10.1177/14771535231169904.

Park, S. *et al.* (2020) ‘Visibility of the phantom array effect according to luminance, chromaticity and geometry’, *Lighting Research & Technology*, 52(3), pp. 377–388. Available at: https://doi.org/10.1177/1477153519867115.

Perenboom, M.J.L. *et al.* (2018) 'Quantifying visual allodynia across migraine subtypes: the Leiden Visual Sensitivity Scale', *Pain*, 159(11), pp. 2375–2382. Available at: https://doi.org/10.1097/j.pain.0000000000001343.

Perz, M. *et al.* (2017) 'Quantifying the Visibility of Periodic Flicker', *LEUKOS - Journal of Illuminating Engineering Society of North America*, 13(3), pp. 127–142. Available at: https://doi.org/10.1080/15502724.2016.1269607.

Perz, M. *et al.* (2018) 'Stroboscopic effect: contrast threshold function and dependence on illumination level', *Journal of the Optical Society of America A*, 35(2), p. 309. Available at: https://doi.org/10.1364/josaa.35.000309.

Perz, M. (2019) *Modelling Visibility of Temporal Light Artefacts*. Available at: https://pure.tue.nl/ws/files/114194362/20190205_Perz.pdf (Accessed: 5 February 2019).

Vogels, I.M.L.C. and Hernando, I. (2012) *Effect of Eye Movements on Perception of Temporally Modulated Light*. Available at: http://2012.experiencinglight.nl/doc/28.pdf.

Wang, L. *et al.* (2017) 'P-141: Phantom Array Effect of LED Lighting', *SID Symposium Digest of Technical Papers*, 48(1), pp. 1804–1807. Available at: https://doi.org/10.1002/sdtp.12037.

Wang, L. *et al.* (2021) 'Dependence of Illumination Level on Phantom Array Effect', *SID Symposium Digest of Technical Papers*, 52(S1), pp. 8–10. Available at: https://doi.org/10.1002/sdtp.14352.

Watson, A.B. (2017) 'QUEST+: A general multidimensional Bayesian adaptive psychometric method', *Journal of Vision*, 17(3), p. 10. Available at: https://doi.org/10.1167/17.3.10.

Wooten, B.R. *et al.* (2010) 'A practical method of measuring the human temporal contrast sensitivity function', *Biomedical Optics Express*, 1(1), p. 47. Available at: https://doi.org/10.1364/BOE.1.000047.

Yan, T. *et al.* (2019) 'THE VISIBILITY OF THE PHANTOM ARRAY EFFECT UNDER OFFICE LIGHTING CONDITION', in *PROCEEDINGS OF the 29th Quadrennial Session of the CIE*. International Commission on Illumination, CIE, pp. 17–21. Available at: https://doi.org/10.25039/x46.2019.OP03.

Yu, X.L. *et al.* (2018) 'INFLUENCE OF FREQUENCY, WAVEFORM AND COLOUR ON THE VISIBILITY OF THE PHANTOM ARRAY EFFECT', in *PROCEEDINGS OF CIE 2018 TOPICAL CONFERENCE ON SMART LIGHTING*. International Commission on Illumination, CIE, pp. 138–146. Available at: https://doi.org/10.25039/x45.2018.OP23.